ISSN 1674-1056
http://cpb.iphy.ac.cn
http://iopscience.iop.org/cpb
中国物理 B
Chinese Physics
中国物理
Chinese Physics B

Effect of oxygen content on dielectric characteristics of Cr-doped $LaTiO_x$

Ming Ma(马铭), Yan Chen(陈彦), Yi-Min Cui(崔益民)
Citation: Chin. Phys. B . 2018, 27(5): 057702. **doi:** 10.1088/1674-1056/27/5/057702

Journal homepage: http://cpb.iphy.ac.cn; http://iopscience.iop.org/cpb

What follows is a list of articles you may be interested in

Indium-tin oxide films obtained by DC magnetron sputtering for improved Si heterojunction solar cell applications

Gu Jin-Hua, Si Jia-Le, Wang Jiu-Xiu, Feng Ya-Yang, Gao Xiao-Yong, Lu Jing-Xiao
Chin. Phys. B . 2015, 24(11): 117703. **doi:** 10.1088/1674-1056/24/11/117703

Stability and elastic properties of Nb_xC_y compounds

Gao Xu-Peng, Jiang Ye-Hua, Liu Yang-Zhen, Zhou Rong, Feng Jing
Chin. Phys. B . 2014, 23(9): 097704. **doi:** 10.1088/1674-1056/23/9/097704

Dielectric loss of half-doped manganite $La_{0.5}Ca_{0.5}MnO_3$

Cao Xian-Sheng, Ji Gao-Feng, Luo Bing-Cheng, Li Feng
Chin. Phys. B . 2013, 22(8): 087702. **doi:** 10.1088/1674-1056/22/8/087702

Effect of oxygen content on dielectric characteristics of Cr-doped $LaTiO_x$*

Ming Ma(马铭)[1], Yan Chen(陈彦)[2,†], and Yi-Min Cui(崔益民)[2]

[1] *School of Aeronautic Science and Engineering, Beihang University, Beijing* 100191, *China*
[2] *School of Physics, Beihang University, Beijing* 100191, *China*

(Received 16 December 2017; revised manuscript received 17 January 2018; published online 26 April 2018)

The ceramics $La_{0.85}Cr_{0.15}TiO_x$ and $La_{0.7}Cr_{0.3}TiO_x$ are prepared by conventional solid-state reaction method. The dielectric properties of Cr-doped $LaTiO_x$ as a function of frequency (0.1 kHz $\leq f \leq$ 1 MHz) and temperature (77 K $\leq T \leq$ 360 K) are studied. The blocks are then annealed in a flowing O_2 or Ar/H_2 to convert their oxygen content and the tests mentioned above are performed. The highly oxygenated samples exhibit extremely high low-frequency dielectric constants at room temperature ($\sim 10^6$). The results show that the oxygen stoichiometry could significantly influence the dielectric properties of Cr-doped $LaTiO_x$.

Keywords: oxygen content, dielectric characteristics, $LaTiO_x$

PACS: 77.84.Bw, 77.22.Gm, 61.72.–y **DOI:** 10.1088/1674-1056/27/5/057702

1. Introduction

Perovskite oxides have been extensively studied in recent years due to their various exotic properties. This is mainly because of their superior properties in dielectric, ferroelectric, piezoelectric, superconductivity, etc.[1–4] Lanthanum titanium oxide (LTO), as an important titanate material, has attracted a great deal of researchers' attention recently.[5] Many researchers have studied LTO materials from different perspectives. For example, Schmehl *et al.* reported the transport properties of $LaTiO_x$ films and heterostructures.[6] Schmitz *et al.* discussed the effect of the experimentally observed Jahn-Teller distortion of the oxygen octahedronin $LaTiO_3$ on the magnetic exchange.[7] Lunkenheimer studied the dielectric properties and dynamical conductivity of $LaTiO_x$ from dc to optical frequencies.[8]

Perovskite has the flexibility of changing the effective negative charges by performing doping substitution on the cationic sites. This class of compound can go through a wide range of structural phase transition, which can strongly affect its physical and chemical properties. Among various types of titanate perovskites, LTO is considered to be a very promising material.[9,10] Cu doping in LTO can not only improve its dielectric properties, but also enhance the Fenton degradation of rhodamine B.[11,12] The Sr doping lowers the conduction band and reduces the band gap of $La_{1-x}Sr_xTiO_3$.[13] As can be seen, the enhancement in total conductivity of the LTO perovskite can be achieved only at lower doping concentration. The opposite effect is observed for higher doping concentration.[14]

The Cr is an important doping element commonly used to improve the properties of the material.[15–17] It has been verified by first-principles calculations that Cr doping improves the conductivity of $LiFePO_4$.[18] The Cr-doped $SrTiO_3$ single crystals exhibit current-driven insulator–conductor transition characteristics which can be used for fabricating the next-generation non-volatile memory devices.[19] In $Li_3V_{2-x}Cr_x(PO_4)_3$/C, the initial specific capacity decreases with the decrease in Cr content at a lower current rate. Under the condition of the moderate Cr doping, both the cycle performance and rate performance have been improved.[20]

Annealing in different atmospheres may change the oxygen content of the material, thereby changing the properties of the material. After deposition annealing, the permittivity and the dielectric Q $(1/\tan\delta)$ of single-phase thin film of $Ba_{0.5}Sr_{0.5}TiO_3$ showed significant changes.[21] Titanium oxide films have better electrical properties after being annealed in oxygen.[22] Polycrystalline $La_{0.67}Ba_{0.33}MnO_3$ bulk samples, which were obtained under the annealing conditions at 700 °C in the flowing 95%Ar:5%H_2(Ar/H_2) mixed gas or a different time, have significantly different insulator–metal transition temperature and AC magnetic susceptibility.[23] Oxygen content can significantly affect the dielectric properties of TiO_2 crystals.[24]

In this study, the Cr-doped $LaTiO_x$ is synthesized using the solid-state method and the samples are annealed in O_2 or Ar/H_2 to change the oxygen content. The effects of Cr-doped ratio and oxygen content on the dielectric properties of Cr-doped $LaTiO_x$ are systematically investigated.

2. Experimental details

The ceramics $La_{0.85}Cr_{0.15}TiO_x$ and $La_{0.7}Cr_{0.3}TiO_x$ were prepared by solid-state reaction. The starting powders La_2O_3,

*Project supported by the National Natural Science Foundation of China (Grant No. 51571006).
†Corresponding author. E-mail: chenyan@buaa.edu.cn
© 2018 Chinese Physical Society and IOP Publishing Ltd

Cr_2O_5, and TiO_2 (with purity $> 99.99\%$) were mixed as required and fired at 1450 °C for 600 min in the air with intermediate grinding in an agate mortar. The grinding and sintering process was repeated three times. Then the mixture was reground, pressed into pellets of 8 mm in diameter and sintered at 1520 °C in the air for another 600 min followed by surface cooling. In order to explore the influence of oxygen content, the samples were annealed at 700 °C in flowing O_2 or Ar/H_2 mixed gas for 60 min and then cooled down.

The structural analysis of the pellet was checked by x-ray diffraction (XRD) using Cu-Kα radiation with 2θ ranging from 20° to 80°. The chemical compositions and chemical states of the as-prepared pellets were characterized by x-ray photoelectron spectroscope (XPS, ESCALAB 250Xi, Thermo Scientific). The silver paste was coated on both sides of the disk as an electrode to test the dielectric properties. The dielectric properties of bulks were measured by a precise impedance analyzer 6500B (Wayne Kerr corp.). The temperature was automatically monitored and controlled by LakeShore temperature controller (Model: 331) with temperature ranging from 77 K to 360 K. Data measurement frequency was in a range from 0.1 kHz to 1 MHz.[25–32]

3. Results and discussion

3.1. Sample characterization

The XRD spectra of Cr-doped $LaTiO_x$ composites at room temperature are shown in Fig. 1. The intensity of the peak varies with the amount of chromium doped and the oxygen content. The analyses of the XRD spectra demonstrate that the lattice structure is tetragonal. For the original sample as shown in Figs. 1(a) and 1(b), except for the 200 peak, the peak intensities increase as the chromium concentration increases. The radius of Lanthanum ion is different from that of Chromium ion,[33] and thus Cr ionis substituted for La ion, the lattice structure of $LaTiO_3$ can be distorted due to the different ionic radii. As shown in Figs. 1(c) and 1(d), comparing with $La_{0.85}Cr_{0.15}TiO_{x+\delta}$, the intensities of the peak (200) and (211) of $La_{0.7}Cr_{0.3}TiO_{x+\delta}$ become weak and some impurity peaks appear. Comparing with the original samples, the intensities of the peaks (211) and (022) become weak after O_2 annealing. As for the Ar/H_2-annealed samples shown in Figs. 1(e) and 1(f), the intensity of peak (200) strengthens but that of (211) peak weakens. The (200) peak and (022) peak intensities become weak after Ar/H_2 annealing. The reason for these results may be that the annealing conditions affect the crystallinity of the sample.[34]

The x-ray photoelectron spectrum (XPS) analysis is also performed to explore the surface chemical compositions of the Cr-doped $LaTiO_x$ samples. The O 1s core level spectra of the prepared samples are displayed in Figs. 2(a)–2(f). In spite of the different annealing atmospheres and doping ratios of the ceramics, it is important to note that the spectra are virtually identical. This assures that in all cases a similar oxygen valence can be estimated at the surface and the change of the dielectric properties with the same doping proportion is mainly attributed to the difference in oxygen concentration.[35–37]

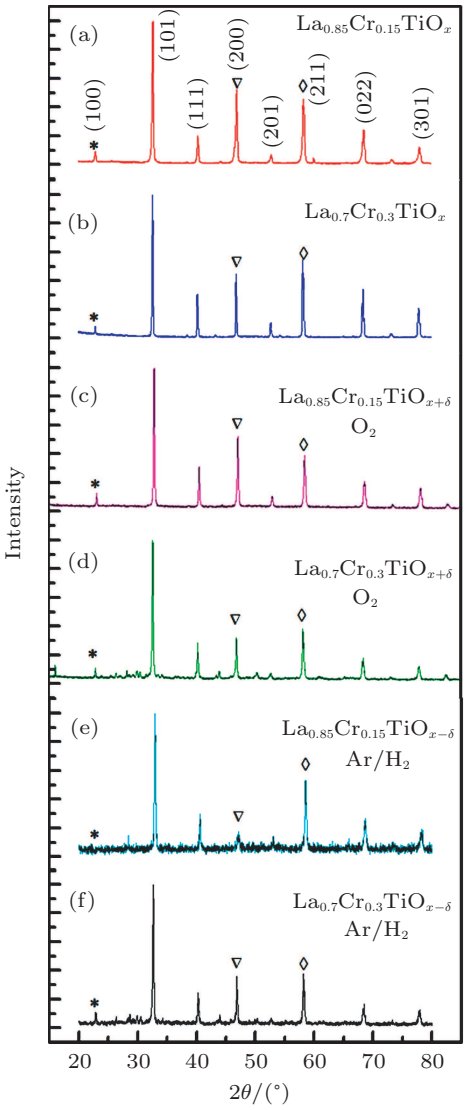


Fig. 1. (color online) XRD spectra for (a) $La_{0.85}Cr_{0.15}TiO_x$, (b) $La_{0.7}Cr_{0.3}TiO_x$, (c) O_2-annealed $La_{0.85}Cr_{0.15}TiO_{x+\delta}$, (d) O_2-annealed $La_{0.7}Cr_{0.3}TiO_{x+\delta}$, (e) Ar/H_2-annealed $La_{0.85}Cr_{0.15}TiO_{x-\delta}$, and (f) Ar/H_2-annealed $La_{0.7}Cr_{0.3}TiO_{x-\delta}$ at room temperature.

Figures 3(a)–3(f) show La 3d states of the perovskite under different oxygen conditions, respectively. The core and the satellite peaks of La $3d_{5/2}$ and La $3d_{3/2}$ each show a clear doublet structure specific for oxides. The primary peaks are located at ~834.62 eV for La $3d_{5/2}$ and ~850.87 eV for La $3d_{3/2}$, respectively. The satellite peaks are around ~838.47 eV and ~855.32 eV, respectively. The energy difference between core and satellite peaks is about 4 eV. The presence of satellite peak La 3d is due to the monopole excitation arising from a change in the screening of the valence electrons upon the removal of a core electron. It is clear that the valence states of La

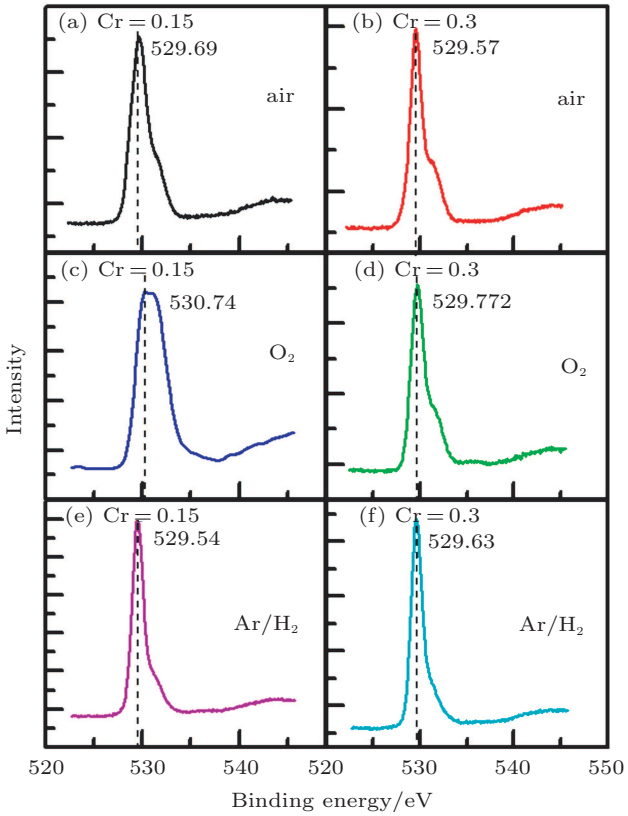


Fig. 2. (color online) O 1s XPS spectra of (a) $La_{0.85}Cr_{0.15}TiO_x$, (b) O_2-annealed $La_{0.85}Cr_{0.15}TiO_{x+\delta}$, (c) Ar/$H_2$-annealed $La_{0.85}Cr_{0.15}TiO_{x-\delta}$, and (d) $La_{0.7}Cr_{0.3}TiO_x$, (e) O_2-annealed $La_{0.7}Cr_{0.3}TiO_{x+\delta}$, and (f) Ar/$H_2$-annealed $La_{0.7}Cr_{0.3}TiO_{x-\delta}$.

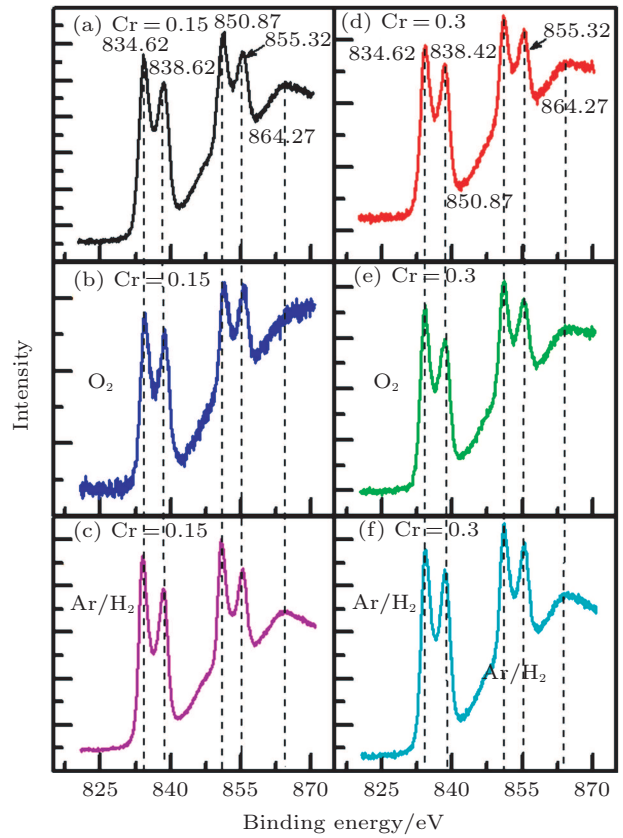


Fig. 3. (color online) La 3d XPS spectra of (a) $La_{0.85}Cr_{0.15}TiO_x$, (b) O_2-annealed $La_{0.85}Cr_{0.15}TiO_{x+\delta}$, (c) Ar/$H_2$-annealed $La_{0.85}Cr_{0.15}TiO_{x-\delta}$, (d) $La_{0.7}Cr_{0.3}TiO_x$, (e) O_2-annealed $La_{0.7}Cr_{0.3}TiO_{x+\delta}$, and (f) Ar/$H_2$-annealed $La_{0.7}Cr_{0.3}TiO_{x-\delta}$.

ions correspond to those of La^{3+}.[35–37] It is important that the valence of La ions do not vary significantly with the difference in oxygen concentration.

The Cr 2p spectra of the samples are exhibited in Fig. 4. It is clear that two peaks at 576.37 eV and 586.17 eV are assigned to the Cr^{3+} $2p_{3/2}$ and Cr^{3+} $2p_{1/2}$ orbits, respectively.[38,39] As for the O_2-annealed ceramic, the peak at about 579.17 is attributed to the $2p_{3/2}$ of Cr^{6+} species,[38] and the peak at 573.17 is assigned to the Cr metal.[38] The reason may be that the electrons around the chromium species combine with the oxygen, which causes the chromium ions to change their valence.

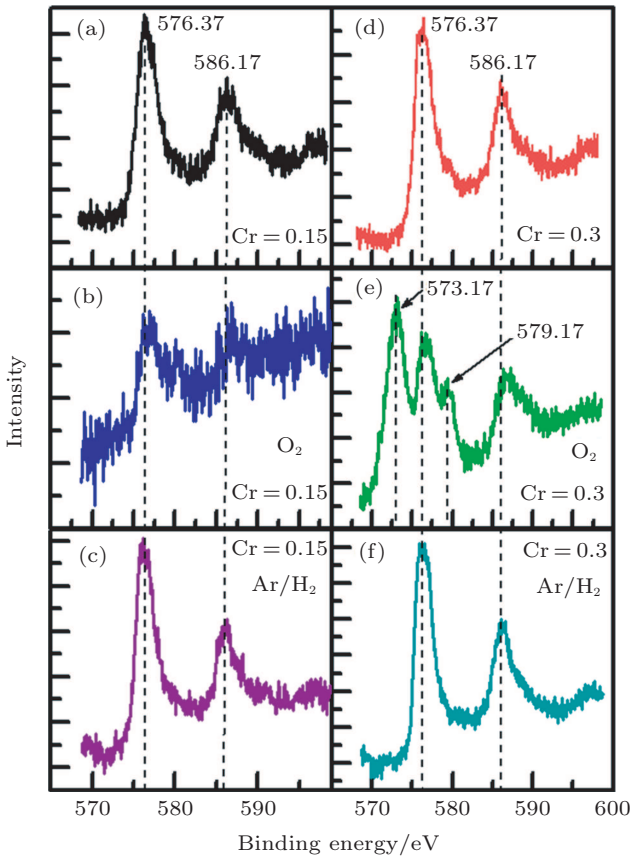


Fig. 4. (color online) Cr 2p XPS spectra of (a) $La_{0.85}Cr_{0.15}TiO_x$, (b) O_2-annealed $La_{0.85}Cr_{0.15}TiO_{x+\delta}$, (c) Ar/$H_2$-annealed $La_{0.85}Cr_{0.15}TiO_{x-\delta}$, (d) $La_{0.7}Cr_{0.3}TiO_x$, (e) O_2-annealed $La_{0.7}Cr_{0.3}TiO_{x+\delta}$, and (f) Ar/$H_2$-annealed $La_{0.7}Cr_{0.3}TiO_{x-\delta}$.

The high-resolution XPS spectra of Ti2p are shown in Fig. 5. Titanium is a more active metal. Its valence is usually bivalent, trivalent, and tetravalent. As shown in Fig. 5, two primary peaks can be explained as a combined effect of surface Ti^{4+} and near-surface Ti^{3+} interstitial defects. In order to further study the influence of oxygen atmosphere on the titanium ions, the measured data are split, which are displayed in Figs. 5(a)–5(f). The symmetric curve with binding energy located at 458.7 eV and 464.3 eV is in accordance with those of Ti^{4+} $2p_{3/2}$ and Ti^{4+} $2p_{1/2}$ in samples, respectively. The two peaks at 457.9 eV and 463.6 eV are assigned to the Ti^{3+} $2p_{3/2}$

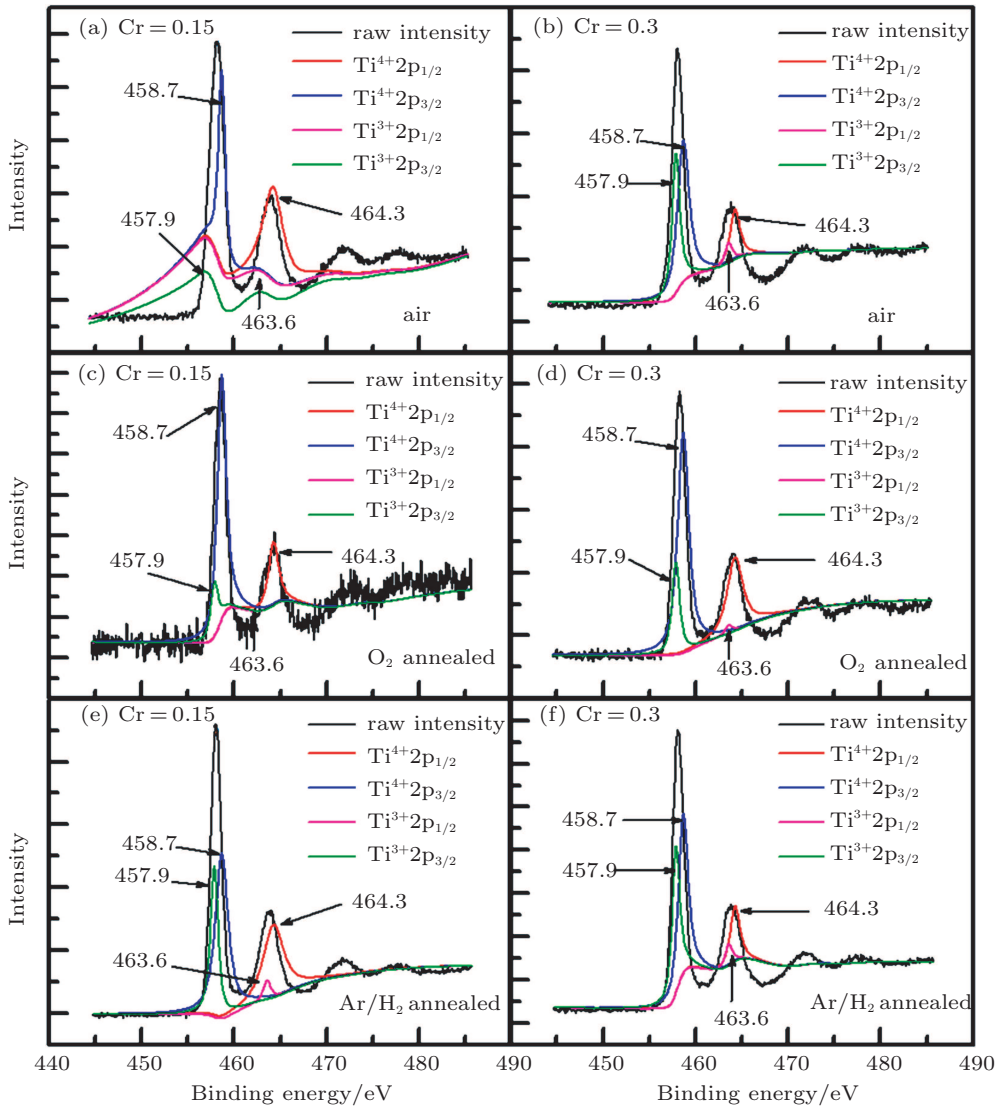


Fig. 5. (color online) Ti 2p XPS spectra of (a) $La_{0.85}Cr_{0.15}TiO_x$, (b) O_2-annealed $La_{0.85}Cr_{0.15}TiO_{x+\delta}$, (c) Ar/$H_2$-annealed $La_{0.85}Cr_{0.15}TiO_{x-\delta}$, (d) $La_{0.7}Cr_{0.3}TiO_x$, (e) O_2-annealed $La_{0.7}Cr_{0.3}TiO_{x+\delta}$, and (f) Ar/$H_2$-annealed $La_{0.7}Cr_{0.3}TiO_{x-\delta}$.

and Ti^{3+} $2p_{1/2}$ orbits, respectively.[40–42] The peak height and area can be used to characterize the proportions of elements. By comparison, it can be seen that the proportion of tetravalent titanium ions in the ceramic annealed in an oxygen atmosphere was the largest. This is due to the binding of titanium ions with oxygen ions, which leads to the lose of electrons.

Finally, the different annealing atmospheres can affect oxygen concentration of the ceramic. However, the valence of oxygen ion is not affected. As shown in Fig. 3, the valence states of La ions remain unchanged. In addition to $La_{0.7}Cr_{0.3}TiO_x$ annealed in oxygen, the valence states of Cr ions remain constant too. Therefore, we believe that the structural stability of the material should be attributed to the difference in concentration of Ti^{4+} ions.

3.2. Dielectric properties

The dielectric constant is a characteristic of material insulation, which indicates the ability of a substance to hold the charge. Figure 6 shows the temperature-sensitive properties of the dielectric constant $\varepsilon^* = \varepsilon' - i\varepsilon''$ (ε^* is the complex permittivity, ε' is the real part and ε'' is the imaginary part of the complex permittivity) of Cr-doped blocks at different frequencies. Figures 6(a) and 6(b) show the temperature dependence of the dielectric constant ε' of the Cr-doped $LaTiO_x$. As shown in Fig. 6(b), the dielectric constant of sample $La_{0.7}Cr_{0.3}TiO_x$ is independent of temperature and frequency at the temperature below 150 K. However, at temperatures above 150 K, the dielectric constant of the sample increases with increasing temperature. For instance, the ε' value increases rapidly as the temperature rises from 150 K to 220 K when the measured frequency is 0.1 kHz. The phenomenon may be caused by thermally exciting more electron–hole pairs when the temperature is over 150 K.[43] As the frequency increases, the ε' value exhibits temperature dependence in higher temperature region. In the temperature range of 220–300 K, the dielectric constant increases slowly as the carrier reaches a saturation state. The ε' value increases rapidly again when the temperature

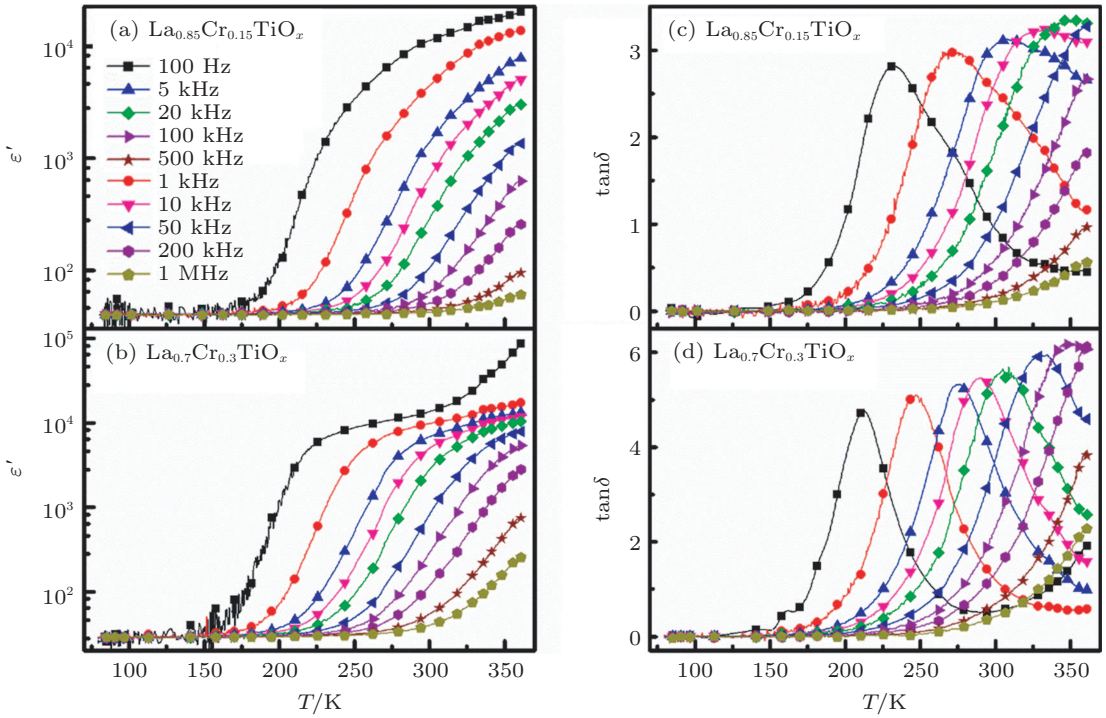


Fig. 6. (color online) Temperature-dependent ε' and $\tan\delta$ values of ((a), (c)) $La_{0.85}Cr_{0.15}TiO_x$ and ((b), (d)) $La_{0.7}Cr_{0.3}TiO_x$ in temperature range from 77 K to 360 K for different frequencies.

is above 300 K, which may be due to another type of carrier that is excited at a temperature above 300 K.[44] The trend of ε' with temperature is also affected by the frequency. According to Figs. 6(a) and 6(b), it can be concluded that the values of dielectric constant ε' increase as the concentration of doped chromium increases. The ε' of the sample turns into an extremely high low-frequency dielectric constants at higher temperature. It increases rapidly with increasing temperature when the temperature is higher than a certain point. The temperature point is also influenced by the chromium concentration.

Figures 6(c) and 6(d) show the dielectric loss tangent $\tan\delta$ ($\tan\delta = \varepsilon''/\varepsilon'$) curves and temperature curves of the samples at different frequencies. For the sample $La_{0.7}Cr_{0.3}TiO_x$, it is shown that the dielectric constant ε' is independent of temperature nor frequency at temperatures below 150 K, which corresponds to the independence of ε' mentioned above. For both samples, if $d(\tan\delta)/dT = 0$ moves toward high temperature as the measured frequency increases, the temperature exhibits a thermal excitation relaxation process.[28–30] The Cr doping ratio has a significant effect on the dielectric loss. The doping of Cr may affect the conductivity and polarization of the sample, both of which determine the dielectric loss of the sample.[43]

It can be concluded that the dielectric constant ε' increases as the concentration of doped chromium increases. The dielectric loss is also significantly affected by the Cr doping ratio. This may be because when chromium ions replace lanthanum ions, the conductivity and the polarizability change, affecting the dielectric constant of the sample.[43]

3.3. Effect of O_2 annealing on dielectric properties

The Cr-doped $LaTiO_x$ is oxidized when annealed in oxygen, which may affect the crystal structures of some types of perovskites, and influence the physical and chemical properties.[21] The bulks are annealed in oxygen and tested as mentioned above. Figures 7(a) and 7(b) show the temperature-dependent ε' values of the oxygen-annealed Cr-doped samples. Figures 7(c) and 7(d) show the variations of dielectric loss tangent $\tan\delta$ with temperature at different frequencies. According to Figs. 6 and 7, for all the samples, the values of dielectric constant ε' and the dielectric loss tangent increase as the concentration of chromium doping rises. By comparing Fig. 6 with Fig. 7, the dielectric constant will increase after oxygen annealing.

In conclusion, the dielectric properties of Cr-doped $LaTiO_x$ can be improved after being annealed in oxygen. It may be due to the fact that the number of activated carriers increases and the structure changes with rising oxygen content.[45–47] The high value of the dielectric constant may be attributed to the close-packed structure of oxygen ions. Oxygen ions with negative charges, because of two excess electrons, are more loosely bound to the nucleus than in a neutral atom or positive ion, so that the ion is readily distorted by an electric field. Also because of the close-packed structure, the number of polarized ions per unit volume is high, so when an electric field was applied, a high polarization increases, which results in a high dielectric constant.[24] In order to demonstrate the effect of oxygen content on the material property, the oxygen content of the material is reduced for further investigation.

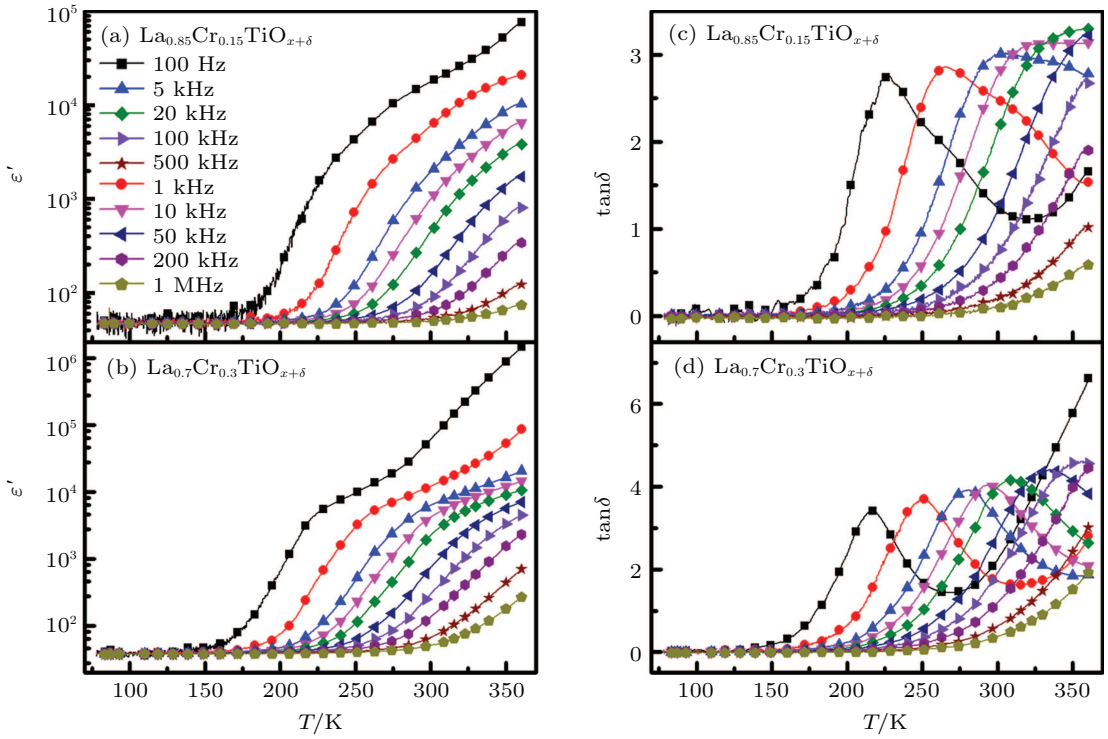


Fig. 7. (color online) Temperature-dependent ε' and $\tan\delta$ values of the oxygen-annealed ((a), (c)) $La_{0.85}Cr_{0.15}TiO_{x+\delta}$ and ((b), (d)) $La_{0.7}Cr_{0.3}TiO_{x+\delta}$ in temperature range from 77 K to 360 K at different frequencies.

The samples are reduced when annealed in Ar/H_2 mixed gas. The oxygen content of the material became lower, which may affect the physical and chemical properties.[21] In order to study the effect of oxygen-deficient on the dielectric property, the samples are annealed in Ar/H_2 and tested as done above. Figures 8(a) and 8(b) show the temperature dependent ε' values and figures 8(c) and 8(d) show the temperature-dependent dielectric loss tangent $\tan\delta$ values of Ar/H_2-annealed samples at different frequencies. According to Figs. 6 and 8, for both samples, the dielectric constant ε' increases as the concentration of doped chromium increases. However, the dielectric constant turns quite different after annealing. Compared

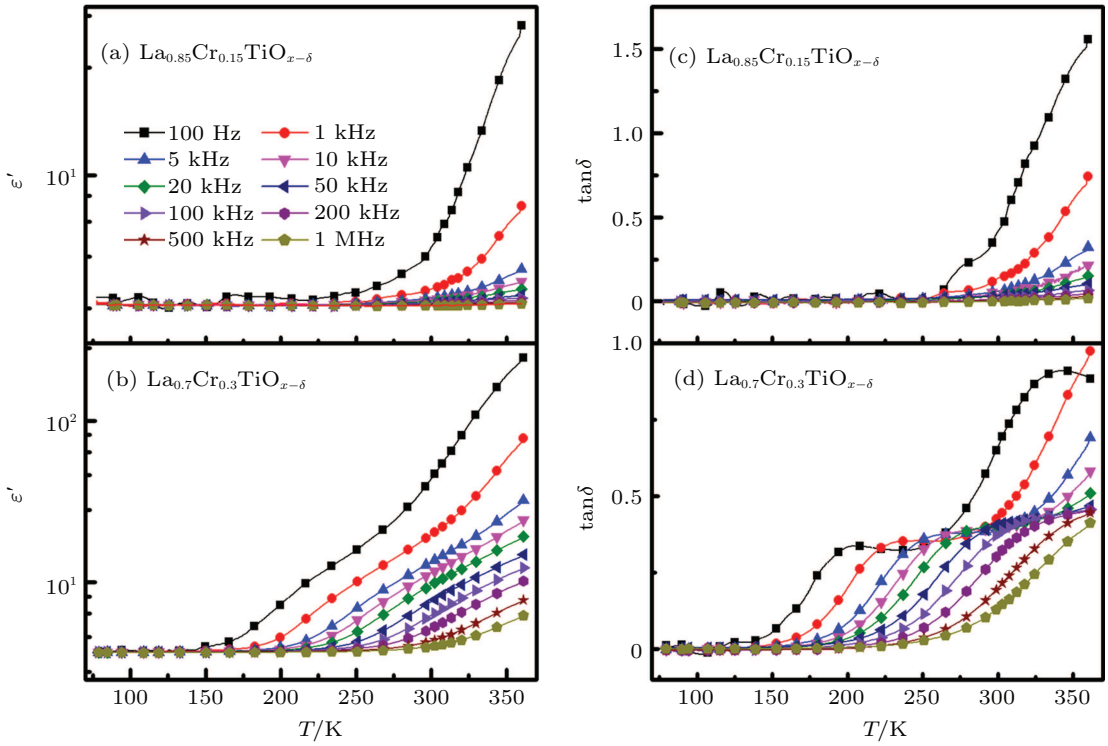


Fig. 8. (color online) Temperature-dependent ε' and $\tan\delta$ values of Ar/H_2-annealed ((a), (c)) $La_{0.85}Cr_{0.15}TiO_{x-\delta}$ and ((b), (d)) $La_{0.7}Cr_{0.3}TiO_{x-\delta}$ in temperature range from 77 K to 360 K at different frequencies.

Fig. 6(a) with Fig. 8(a), the dielectric constant ε' values of the original samples will show obvious temperature dependence when the temperature is above 160 K, while those for theAr/H_2-annealed samples are 240 K. The ε' increases rapidly with increasing temperature when the temperature is higher than a certain point. The temperature point becomes higher after the sample has been annealed in Ar/H_2. A comparison between Figs. 6(b) and 8(b) shows that the non-annealed sample exhibits a very high low-frequency dielectric constant at room temperature and the low-frequency dielectric constant of the annealed sample does not exceed 2×10^3. The dielectric constant of the $La_{0.7}Cr_{0.3}TiO_x$ after being annealed is also much smaller.

A comparison of Fig. 6 with Fig. 8 shows that the dielectric loss tangent values of the samples with two different doping ratios decrease. As shown in Fig. 8(d), only the 0.1 kHz frequency curve has a maximum value over the tested temperature range. Both curves of non-annealed $La_{0.85}Cr_{0.15}TiO_x$ and $La_{0.7}Cr_{0.3}TiO_x$ exhibit their maximum values, while the curves of Ar/H_2-annealed samples each have only one extreme value. It is assumed that extreme point will appear in the high-temperature region. In conclusion, the dielectric loss tangent decreases, and most of the extreme value points disappear in the test temperature range. This may be due to the decrease in the number of activated carriers and the increase in the temperature at which the carriers are activated after Ar/H_2-annealing.

A series of distinct phases with variable oxygen stoichiometry exists in the Cr-doped $LaTiO_x$ system. Starting with fully oxidized compounds, the oxygen content is then reduced and the perovskite-related structure changes. The structural and physical properties vary drastically as oxygen quantity becomes stoichiometric.[47] In the Ar/H_2-annealed samples, due to the low oxygen content, vacancies are formed in the samples. Charges trapped by the vacancies cannot participate in the long-distance conduction, but form a space charge. Many oxygen vacancies exist in the sample with low oxygen content, which can capture carriers. At lower voltage, most of the charges injected from the electrode fill the vacancies and cannot participate in the electrical conductivity resulting in a decrease in dielectric constant. For samples with high oxygen content, the oxygen vacancies are less and the oxygen ions are tightly linked, most of the charges are involved in the conductance. Due to the close-packed structure of oxygen ions, the number of polarizable ions is high. When an electric field is applied, a high polarization is established, resulting in a high dielectric constant. Space charges limit the current, thus dielectric loss varies with oxygen content. The current density decreases as the oxygen content decreases, resulting in a decrease in dielectric loss. This also shows that under the experimental conditions, the dielectric loss is determined mainly by the macroscopic charge transfer.[24,48]

The oxygen ions (O^{2-}) act as a bridge between Ti^{3+} and Ti^{4+} and play an essential role in the Ti^{3+}–O_2–Ti^{4+} superexchange interaction. Naturally, the extent to which the number of oxygen ions changes makes the crystal lattice structure collapse down, so the dielectric property of the material changes significantly.

4. Conclusions

In summary, doped Cr ion concentration can significantly influence the dielectric property of the LTO. The doping ratio increases from 15% to 30%, the dielectric constant is increased by almost an order of magnitude. Annealing in flowing O_2 or Ar/H_2 can change the oxygen content and influence the dielectric properties of the samples. The sample with high oxygen content shows higher dielectric constant, which means that O_2 annealing is an effective method to improve the dielectric characteristics of Cr-doped LTO.

References

[1] Ahn C H, Triscone J M and Mannhart J 2003 *Nature* **424** 1015
[2] Cheng J G, Meng X J, Li B, Tang J, Guo S L and Chu J H 1999 *Appl. Phys. Lett.* **75** 2132
[3] Maurya D, Pramanick A, An K and Priya S 2012 *Appl. Phys. Lett.* **100** 172906
[4] Suzuki H, Bando H, Ootuka Y, Inoue I, Yamamoto T, Takahashi K and Nishihara Y 1999 *J. Phys. Soc. Jpn.* **65** 1529
[5] Moetakef P, Zhang J Y, Kozhanov A, Jalan B, Seshadri R, Allen S J and Stemmer S 2011 *Appl. Phys. Lett.* **98** 112110
[6] Schmehl A, Lichtenberg F, Bielefeldt H, Mannhart J and Schlom D G 2003 *Appl. Phys. Lett.* **82** 3077
[7] Schmitz R, Entin-wohlman O, Aharony A, Harris A B and Mueller-hartmann E 2005 *Phys. Rev. B* **71** 144412
[8] Lunkenheimer P, Rudolf T, Hemberger J, Pimenov A, Tachos S, Lichtenberg F and Loidl A 2003 *Phys. Rev. B* **68** 245108
[9] Madhavan B and Ashok A 2015 *J. Sol-Gel Sci. Technol.* **73** 1
[10] Fasquele D, Carru J C, Gendre L L, Paven C L, Pinel J, Cheviré F, Tessier F and Marchand R 2005 *J. Eur. Ceram. Soc.* **25** 2085
[11] Chen Y, Xu J X, Cui Y M, Shang G Y, Qian J Q and Yao J E 2016 *Prog. Nat. Sci.: Mater. Int.* **26** 158
[12] ZhangL L, Nie Y L, Hu C and Qu J H 2012 *Appl. Catal. B* **125** 418
[13] Gao L H, Ma Z and Fan Q B 2011 *J. Electroceram.* **27** 114
[14] Bradha M, Hussain S, Chakravarty S, Ashok A and Amarendra G 2014 *Ionics* **20** 1343
[15] Kim J K, Sang S S and Kim W J 2006 *Appl. Phys. Lett.* **88** 132901
[16] Janousch M, MeijerG I, Staub U, Delley B, Karg S F and Andreasson B P 2007 *Adv. Mater.* **19** 2232
[17] Borgarello E, Kiwi J, Graetzel M, Pelizzetti E and Visca M 1982 *J. Am. Chem. Soc.* **104** 2996
[18] Shi S, Liu L, Ouyang C, Wang D S, Huang X J and Chen L Q 2003 *Phys. Rev. B* **68** 195108
[19] Watanabe Y, Bednorz J G, Bietsch A, Gerber C, Widmer D and Beck A 2001 *Appl. Phys. Lett.* **78** 3738
[20] Chen Y H, Zhao Y M, An X N, Liu J M, Dong Y Z and Chen L 2009 *Electrochim. Acta* **54** 5844
[21] ChangW, Horwitz J S, Carter A C, Pond J M, Kirchoefer SW, Gilmore C M and Chrisey D B 1999 *Appl. Phys. Lett.* **74** 1033
[22] Lee M K, Huang J J and Wu T S 2005 *Semicond. Sci. Technol.* **20** 519
[23] Cui Y M, Zhang L W, Wang C C, Shi K and Cao B S 2006 *J. Magn. Magn. Mater.* **297** 21
[24] Bamzai K K, Koohpayeh S M, Kaur B, Fort D and Abell J S 2008 *Ferroelectrics* **377** 1
[25] Cui Y M and Wang R M 2007 *Appl. Phys. Lett.* **91** 233513
[26] Cui Y M, Cai W, Li Y, Qian J Q, Xu P, Wang R M and Yao J E 2006 *J. Appl. Phys.* **100** 034101
[27] Chen C, Xu K B, Cui Y M and Wang C C 2012 *Mater. Lett.* **89** 153
[28] Lu C and Cui Y M 2012 *Physica B* **407** 3856

[29] Xu J X and Cui Y M 2013 *Mater. Sci. Eng. B* **178** 316
[30] Cui Y M, Zhang L W, Xie C L and Wang R M 2006 *Solid State Commun.* **138** 481
[31] Cui Y M, Zhang L W and Wang R M 2006 *Physica C* **442** 29
[32] Cui Y M, Liu W and Wang R M 2013 *Phys. Chem. Chem. Phys.* **15** 6804
[33] Jr E R N 1959 *Biochim. Biophys. Acta* **63** 1381
[34] Vidyasagar C C, Muralidhara H B, Naik Y A, Gururaj H and Ilango M S 2015 *Energy Environ. Focus* **4** 54
[35] López G P, Castner D G, Ratner B D 1991 *Surf. Interface Anal.* **17** 267
[36] Miao J P, Lü Z, Li L P, Ning F L, Liu Z G, Huang X Q, Sui Y, Qian Z N, Su W H 2000 *Mater. Lett.* **427** 267
[37] Marshall M S J, Newell D T, Payne D K, Egdell R G and Castell M R 2011 *Phys. Rev. B* **83** 035410
[38] Daulton T L and Little B J 2006 *Ultramicroscopy* **106** 561
[39] Zhong L, Cai W and Zhong Q 2014 *Rsc Adv.* **4** 43529
[40] Drera G, Salvinelli G, Brinkman A, Huijben M, Koster G, Hilgenkamp H, Rijnders G, Visentin D and Sangaletti L 2012 *Phys. Rev. B* **87** 1081
[41] Zhou Y, Chen C H, Wang N N, Li Y Y and Ding H M 2016 *J. Phys. Chem. C* **120** 6116
[42] Guillemot F, Porte M C, Labrugere C and Baquey C H 2002 *J. Colloid Interface Sci.* **255** 75
[43] Dholam R, Patel N, Adami M and Miotello A 2009 *Int. J. Hydrogen Energy* **34** 5337
[44] Pesci F M, Wang G, KlugDR, Li Y and Cowan A J 2013 *J. Phys. Chem. C* **117** 25837
[45] Wang G J, Wang C C, Huang S G, Lei C M, Mei J Y, Sun X H and Li T 2012 *J. Electroceram.* **28** 172
[46] Zhang Y T, Wang C C and He M 2009 *J. Phys. D: Appl. Phys.* **42** 055309
[47] Lichtenberg F, Widmer D, Bednorz J G, Williams T and Reller A 1991 *Z. Phys. B* **82** 211
[48] Chang F G, Song G L, Fang K and Wang Z K 2007 *Acta Phys. Sin.* **56** 6068